28 April 2000

ELSEVIER

Chemical Physics Letters 321 (2000) 205–215

CHEMICAL PHYSICS LETTERS

www.elsevier.nl/locate/cplett

Symmetry principles for the design of radiofrequency pulse sequences in the nuclear magnetic resonance of rotating solids

Marina Carravetta [a], Mattias Edén [b], Xin Zhao [a], Andreas Brinkmann [a], Malcolm H. Levitt [a,*]

[a] *Physical chemistry division, Arrhenius Laboratory, Stockholm University, S-106 91 Stockholm, Sweden*
[b] *Department of Chemistry, University of Illinois in Chicago, Chicago, IL 60607-7061, USA*

Received 20 December 1999; in final form 24 February 2000

Abstract

Some new symmetry theorems are presented which simplify the task of designing multiple-pulse radio-frequency pulse sequences in magic-angle-spinning solid-state NMR. The symmetry theorems apply to sequences denoted $\mathrm{R}N_n^\nu$, which consists of N repetitions of a pulse sequence element R, alternating in phase between the values $\pm\pi\nu/N$. Each R element ideally rotates the spins by an angle π about the rotating frame x-axis. The entire $\mathrm{R}N_n^\nu$ sequence is timed to span n rotational periods. Applications are presented for homonuclear double-quantum and zero-quantum recoupling, heteronuclear decoupling and heteronuclear recoupling.

1. Introduction

Magic-angle-spinning (MAS) is an essential technique in the NMR of disordered solids. The sample is rotated rapidly about an axis subtending the 'magic angle' $\tan^{-1}\sqrt{2}$ with respect to the main field, in order to increase the sensitivity and resolution by averaging out chemical shift anisotropies (CSA) and through-space dipole–dipole couplings. In many cases, the magic-angle rotation is accompanied by resonant radio-frequency (rf) fields, in order to enhance the averaging effect of the sample rotation, or sometimes to inhibit it. For example, in heteronuclear *decoupling* [1–5], the rf fields are applied at the Larmor frequency of one spin species in order to reduce their influence on a second spin species, whose signal is observed. In the case of *recoupling* [6–17], the rf fields restore the effect of the dipolar couplings by the magic angle rotation over a limited time interval. This makes it possible to estimate spin-spin distances [11–16] and to excite multiple quantum coherencies [6–10,18,19].

The design of rf pulse sequences in the presence of sample rotation is a complex problem with many possible solutions. Our group has exploited symmetry arguments in order to simplify this task. In previous papers [2,7,10] we have proposed sequences based on a symmetry denoted in general $\mathrm{C}N_n^\nu$. The *symmetry class* of the sequence is specified by three *symmetry numbers* N, n and ν, which are integers. Such sequences have the following properties: (i) they are based on a rf pulse sequence element denoted C, which is a rf cycle, meaning that the rf

* Corresponding author. Fax: +46-8-152187, e-mail: mhl@physc.su.se

0009-2614/00/$ - see front matter
PII: S0009-2614(00)00340-7

fields return the irradiated spins to their initial states in the absence of other interactions; (ii) the duration of each C element is given by $\tau_C = n\tau_r/N$, where $\tau_r = |2\pi/\omega_r|$ is the rotational period of the sample and ω_r is the angular spinning frequency. This implies that N contiguous C elements span exactly n rotational periods; (iii) the phases of consecutive elements differ by the angle $2\pi\nu/N$, i.e. $CN_n^\nu = (C^0)_{\phi_0}(C^0)_{\phi_1}\ldots(C^0)_{\phi_{N-1}}$ where the phases of the elements are $\phi_q = 2\pi q\nu/N$.

In Ref. [2], we showed that the symmetry CN_n^ν implies the following selection rules for the components of the average Hamiltonian [20]:

$$\overline{\mathscr{H}}^{(1)}_{lm\lambda\mu} = 0 \quad \text{if} \quad mn - \mu\nu \neq NZ, \tag{1}$$

$$\overline{\mathscr{H}}^{(2)}_{l_2 m_2 \lambda_2 \mu_2; l_1 m_1 \lambda_1 \mu_1} = 0$$

$$\text{if} \quad \begin{cases} m_1 n - \mu_1 \nu \neq NZ \\ \quad \text{and} \\ m_2 n - \mu_2 \nu \neq NZ \\ \quad \text{and} \\ (m_2 + m_1) n - (\mu_2 + \mu_1)\nu \neq NZ \end{cases} \tag{2}$$

where Z is any integer, l refers to the spatial rotational rank and λ indicates the rank with respect to rotations of the spin polarizations by the resonant rf field. The component indices m and μ take values $m = -l, -l+1, \ldots, +l$ and $\mu = -\lambda, -\lambda+1, \ldots, +\lambda$. The average Hamiltonian terms are defined in Ref. [2].

The spin interactions are conveniently classified according to their ranks l and λ. For example, the isotropic chemical shift has $l = 0$, $\lambda = 1$; the chemical shift anisotropy (CSA) and heteronuclear dipolar coupling both have $l = 2$, $\lambda = 1$; the homonuclear through-space dipolar coupling has $l = 2$, $\lambda = 2$; the homonuclear J-coupling has $l = 0$, $\lambda = 0$. All terms with $l = 2$ and $m = 0$ vanish for the case of exact magic angle spinning. Explicit expressions for the terms are given in Ref. [1].

The selection rules (1) and (2) may be used to construct rotor-synchronized pulse sequences with desirable properties. For example, the symmetries $C7_2^1$ [7–9], $C7_5^{-1}$ [9,10], $C7_1^{-3}$ and $C14_4^{-5}$ [10] suppress all $\overline{\mathscr{H}}^{(1)}_{lm\lambda\mu}$ terms with $0 < l \leqslant 2$ except for $\overline{\mathscr{H}}^{(1)}_{2122}$ and $\overline{\mathscr{H}}^{(1)}_{2-12-2}$. As a result, these sequences provide CSA-compensated double-quantum homonuclear dipolar recoupling.

In addition, a set of symmetries, including $C12_2^1$, may be used for heteronuclear decoupling in the presence of MAS [2]. These symmetries eliminate all terms of the form $\overline{\mathscr{H}}^{(1)}_{2m1\mu}$, retaining some homonuclear dipole–dipole coupling terms of the form $\overline{\mathscr{H}}^{(1)}_{2m2\mu}$, and allowing a relatively small number of heteronuclear cross terms $\overline{\mathscr{H}}^{(2)}_{2m_2 1\mu_2; 2m_1 1\mu_1}$ and $\overline{\mathscr{H}}^{(2)}_{2m_2 2\mu_2; 2m_1 1\mu_1}$.

2. New pulse sequence symmetries

In this Letter, we report a new class of symmetrical rotor-synchronized pulse sequences, denoted RN_n^ν. These sequences are constructed as follows: (i) Select a pulse sequence element R, which rotates resonant spins by π around the x-axis, in the absence of other interactions. This element has an idealized propagation operator of the form:

$$U_R = \exp(-i\pi S_x), \tag{3}$$

where S_x is the x angular momentum operator of the irradiated spin species. In practice, R is equal to a single π pulse or a composite π pulse, as in solution-state heteronuclear decoupling [21]. (ii) Choose an appropriate ratio of rf field to spinning frequency so that the duration of R is equal to $\tau_R = n\tau_r/N$, where N is an even integer. (iii) Derive the sequence R′ by changing the sign of all rf phases in R. Note that R and R′ are identical if they only employ phase-shifts equal to integer multiples of π. (iv) Concatenate R and R′ elements in a phase-shifted alternating sequence of the form:

$$RN_n^\nu = (R)_\phi (R')_{-\phi} (R)_\phi (R')_{-\phi} \ldots (R')_{-\phi}, \tag{4}$$

where

$$\phi = \frac{\pi\nu}{N}. \tag{5}$$

The entire sequence of $N/2$ contiguous RR′ pairs spans exactly n rotational periods. The phase alternation in Eq. (4) resembles the two-pulse phase modulated (TPPM) sequences used in heteronuclear de-

coupling [5]. This relationship will be explored further below.

In a forthcoming publication, we show that $\mathrm{R}N_n^\nu$ symmetry implies the following selection rules for the average Hamiltonian terms:

$$\overline{\mathscr{H}}^{(1)}_{lm\lambda\mu} = 0 \quad \text{if} \quad mn - \mu\nu \neq \frac{N}{2}Z_\lambda , \tag{6}$$

$$\overline{\mathscr{H}}^{(2)}_{l_2 m_2 \lambda_2 \mu_2 ; l_1 m_1 \lambda_1 \mu_1} = 0$$

$$\text{if} \begin{cases} m_1 n - \mu_1 \nu \neq \dfrac{N}{2} Z_{\lambda_1} \\ \quad \text{and} \\ m_2 n - \mu_2 \nu \neq \dfrac{N}{2} Z_{\lambda_2} \\ \quad \text{and} \\ (m_2 + m_1) n - (\mu_2 + \mu_1)\nu \neq \dfrac{N}{2} Z_{\lambda_2 + \lambda_1} \end{cases} \tag{7}$$

The symbol Z_λ indicates any integer with the same parity as λ, i.e. if λ is odd, then Z_λ is any odd integer; if λ is even, then Z_λ is any even integer, including zero.

If the individual R elements only involve phase shifts in multiples of π (amplitude modulation), then rf inhomogeneity terms may also be embedded in the selection rules (6) and (7) by using a term with $l = 0$, $\lambda =$ even and $\mu = \pm 1$. The following discussion assumes amplitude modulated R elements throughout.

The $\mathrm{R}N_n^\nu$ selection rules (6) and (7) are similar but not identical to the $\mathrm{C}N_n^\nu$ selection rules (1) and (2). In particular, the $\mathrm{R}N_n^\nu$ selection rules depend on the spin rotational rank λ, while the $\mathrm{C}N_n^\nu$ selection rules do not. This allows $\mathrm{R}N_n^\nu$ sequences to discriminate between spin interactions on the basis of the parity of the spin rotational rank λ, which creates many new possibilities.

3. Double-quantum homonuclear recoupling

The selection rules (6) and (7) may be used to design pulse sequences which accomplish chemical shift compensated double quantum homonuclear recoupling. For example, the symmetry $\mathrm{R}14_2^6$ suppresses all $\overline{\mathscr{H}}^{(1)}_{lm\lambda\mu}$ terms with $0 < l \leqslant 2$, except for $\overline{\mathscr{H}}^{(1)}_{212-2}$ and $\overline{\mathscr{H}}^{(1)}_{2-122}$. This leads to an average Hamiltonian of the form:

$$\overline{\mathscr{H}}^{(1)} = \sum_{j<k} \left(\omega_{jk} T^{jk}_{2-2} + \omega^*_{jk} T^{jk}_{22} \right), \tag{8}$$

where $T^{jk}_{2\pm 2}$ are second-rank spin operators for the interaction between spins j and k and the magnitude $|\omega_{jk}|$ is independent of the Euler angle γ_{MR}, representing the orientation of the molecules in the rotor-fixed frame [7,8]. This leads to the same basic properties as for the $\mathrm{C}7_2^1$-based sequences, including the maximum double-quantum filtering efficiency of 73% [7]. The choice of the element R is entirely free within the constraint of Eq. (3) and must be chosen according to the magnitude of the symmetry-allowed interactions and robustness with respect to resonance offsets. So far, we have explored the element $\mathrm{R}^0 = (\pi/2)_0(3\pi/2)_\pi$, which is relatively simple and broadband. Written explicitly, the $\mathrm{R}14_2^6$ sequence is given by:

$$\mathrm{R}14_2^6 = \left\{ (90)_{77.1}(270)_{257.1}(90)_{282.9}(270)_{102.9} \right\}^7 \tag{9}$$

(using degrees to denote flip angles and phases), where each $\pi/2$ pulse has a duration $\tau_r/28$, and the rf amplitude corresponds to a nutation frequency equal to 7 times the spinning frequency. The superscript 7 on the right hand side of Eq. (9) indicates 7 repetitions of the bracketed elements, spanning a total of 2 rotational periods. The rf amplitude requirements of this sequence are exactly the same as for implementations of $\mathrm{C}7_2^1$ employing the standard cycles $\mathrm{C} = (360)_0(360)_{180}$ [7] or $\mathrm{C} = (90)_0(360)_{180}(270)_0$ [8]. The dipole–dipole scaling factor of the $\mathrm{R}14_2^6$ sequence, as defined in Ref. [10], is given by $|\kappa| = 0.172$, which is slightly larger than that of the $\mathrm{C}7_2^1$ sequences, $|\kappa| = 0.155$ [10].

In Fig. 1 we use numerical simulations to compare the performances of $\mathrm{R}14_2^6$ with two implementations of the $\mathrm{C}7_2^1$ sequence [7,8] and the CMR7 supercycle proposed by Rienstra et al. [9]. The simulation parameters are typical for a pair of directly-bonded olefinic $^{13}\mathrm{C}$ sites, at a magnetic field of 9.4 T and a spinning frequency $\omega_r/2\pi = 5.5$ kHz.

Fig. 1a shows the predicted double-quantum filtering (2QF) efficiency, as defined in Ref. [8], as a

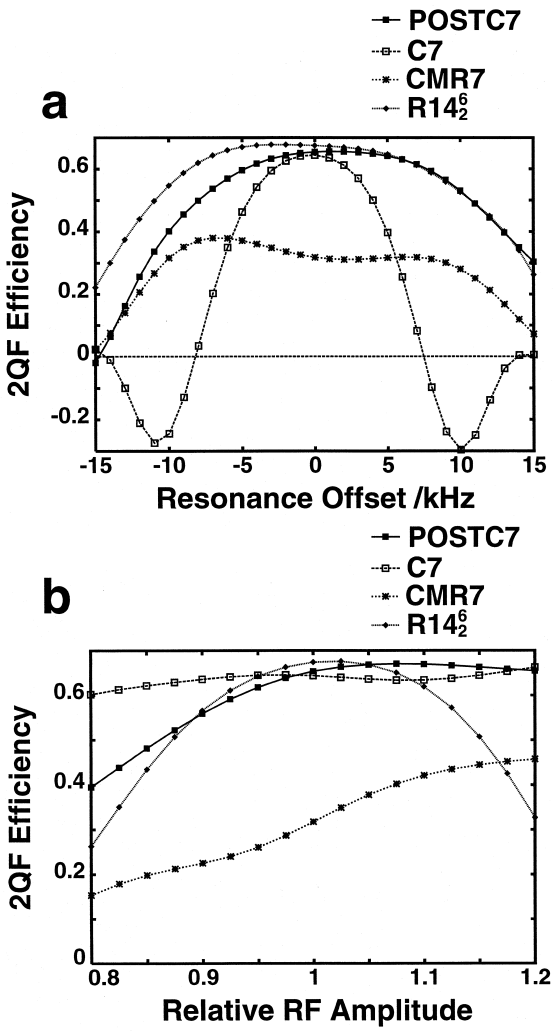

Fig. 1. Simulated double-quantum filtering (2QF) efficiencies of four different recoupling sequences, using parameters corresponding to [2,3-$^{13}C_2$]-diammonium fumarate at a magnetic field of 9.4 T and a spinning frequency of $\omega_r/2\pi = 5.5$ kHz. The dipole–dipole coupling was $b_{IS}/2\pi = -3350$ Hz. The CSA tensors of the two sites were assumed to have the same principal axis system, with the least shielded axis in the HCCH plane and perpendicular to the C–C bond and with the most shielded axis perpendicular to this plane [35]. The CSA parameters for both sites (deshielding convention) were $\delta^{aniso} = 94.17$ ppm, $\eta = 0.59$. (a) 2QF efficiency as a function of resonance offset. The simulations used the nominal rf amplitude, corresponding to the ^{13}C nutation frequency $|\omega_{nut}^{nom}/2\pi| = 38.5$ kHz. (b) 2QF efficiency using on-resonance irradiation against $\omega_{nut}^{S}/\omega_{nut}^{nom}$, i.e. the ratio of the rf field amplitude to its nominal value, at zero resonance offset. The duration of 2Q excitation and reconversion intervals were optimized for each sequence individually and were 364 μs (POSTC7, C7 and R14$_2^6$) and 519 μs (CMR7).

function of the offset of the ^{13}C carrier from the isotropic shift frequency (which is the same for the two sites). As may be seen, R14$_2^6$ and POST-C7 [8] are significantly better than the others, with R14$_2^6$ having a slightly higher simulated efficiency. The CMR7 sequence [9] performs rather poorly with this parameter set, presumably because it is not very robust with respect to chemical shift anisotropy.

Fig. 1b shows the simulated performance of the sequences when the rf amplitude is varied. The C7 sequence is highly robust with respect to this parameter, since each C element is internally-compensated for rf errors. The R14$_2^6$ sequence is more sensitive to the setting of the rf field, but is still quite tolerant to variations in the range $\pm 5\%$. The R14$_2^6$ sequence employs phase shifts of $\pm 77.1°$ between consecutive R elements, implying that adjacent pairs of R elements have nearly opposite phases and combine to achieve an approximate internal compensation for rf field errors. In addition, the R14$_2^6$ symmetry eliminates all cross-terms between rf-inhomogeneity and chemical shifts, in the case of amplitude-modulated R elements. The insensitivity of R14$_2^6$ with respect to chemical shift anisotropy may be understood by examining the structure of the higher order terms. Analysis of the selection rule (7) shows that there are 16 symmetry-allowed terms of the type $\overline{\mathscr{H}}^{(2)}_{2m_2 1\mu_2;2m_1 2\mu_2}$ (CSA × DD cross terms) for R14$_2^6$, while there are 54 such terms for C7$_2^1$.

These good features have been borne out by experiments. Fig. 2 shows experimental 2QF efficiencies for diammonium [2,3-$^{13}C_2$]-fumarate, at a field of 9.4 T and a spinning frequency of $|\omega_r/2\pi| = 5.5$ kHz. The double quantum filtration experiment was implemented as described in Ref. [7], but using a R14$_2^6$ sequence instead of a C7$_2^1$ sequence. The ^{13}C nutation frequency during recoupling was 38.5 kHz in all experiments. The ^1H decoupling field corresponded to a nutation frequency of 110 kHz during the recoupling sequences. As may be seen, the R14$_2^6$ sequence gives a slightly higher 2Q filtering efficiency than POST-C7 under optimal conditions. The experimental maximum double-quantum efficiency is 50%, which is respectable for a compound with large CSA at a reasonably high magnetic field.

Fig. 2b shows that the R14$_2^6$ sequence is also more robust than POST-C7 with respect to rf ampli-

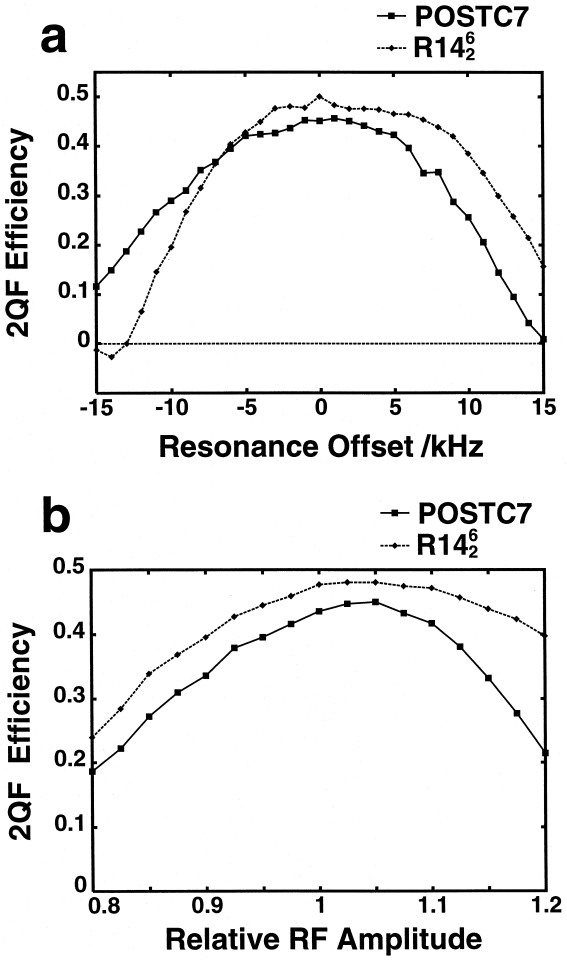

Fig. 2. Experimental ^{13}C 2QF efficiencies for a powder of 99% labelled [2,3-$^{13}C_2$]-diammonium fumarate at a magnetic field of 9.4 T and a spinning frequency $\omega_r/2\pi = 5.5$ kHz, using a filled 4 mm zirconia rotor and a Chemagnetic Infinity-400 spectrometer. The ^{13}C and ^{1}H rf amplitudes during the recoupling sequences corresponded to nutation frequencies of $|\omega^S_{nut}/2\pi| = 38.5$ kHz and $|\omega^I_{nut}/2\pi| = 110$ kHz, respectively. The duration of excitation and reconversion intervals were 364 μs for both POSTC7 and R14$^6_2$. (a) 2QF efficiency as a function of resonance offset. (b) 2QF efficiency as a function of the rf amplitude at zero resonance offset.

tude changes, under these conditions. This behavior does not correlate well with the simulated predictions in Fig. 1b, and is not well understood at present.

There are numerous other solutions for CSA-compensated double quantum recoupling, including R14$^1_2$, R12$^1_2$, R12$^5_2$, R14$^5_4$, R14$^2_4$. A total of 14 inequivalent symmetries has been found in the range $N \leqslant 20, n \leqslant 5$. All of these solutions are compensated for CSA, isotropic chemical shifts and rf inhomogeneity, to first order in the average Hamiltonian and eliminate all second-order cross terms involving CSA and rf inhomogeneity. There are no CN^ν_n sequences which have these properties on the basis of symmetry alone. Simulations indicate that the sequence R12$^5_2$ with R = $(60)_0(300)_{180}(60)_0$ [22] is also very promising. Solutions such as R14$^5_4$ are likely to allow operation at very high spinning frequency.

4. Recoupling of CSA and heteronuclear dipolar interactions

The chemical shift anisotropy interaction may be recoupled by engineering an average Hamiltonian of the form

$$\overline{\mathscr{H}}^{(1)} = \sum_j \left(\omega_j T^j_{1-1} - \omega^*_j T^j_{11} \right), \tag{10}$$

where $T^j_{1\pm1}$ are single-quantum irreducible spherical tensors of rank 1 and ω_j is proportional to the chemical shift anisotropy of spin j. In addition, it is desirable that the magnitude of the recoupled interaction is independent of the Euler angle γ_{MR}. This type of average Hamiltonian may be engineered, at the same time as first-order suppression of homonuclear dipole–dipole coupling terms, isotropic chemical shifts and rf inhomogeneity terms, by using symmetries such as R10$^3_1$, R18$^7_1$, R14$^3_2$, R10$^{-1}_3$, R12$^{-4}_5$. All of these symmetries suppress all relevant first-order terms except $\overline{\mathscr{H}}^{(1)}_{221-1}$ and $\overline{\mathscr{H}}^{(1)}_{2-211}$. In total, 18 inequivalent RN^ν_n symmetries have been found with $N \leqslant 20$ and $n \leqslant 5$. These sequences are likely to be useful for measuring the magnitudes of CSA tensors in heavily-labelled systems.

These same sequences may be used for recoupling heteronuclear dipolar interactions, if they are only applied to one of the spin species. If the species I is irradiated, the recoupled Hamiltonian has the form

$$\overline{\mathscr{H}}^{(1)} = \sum_j \left(\omega_j T^j_{1-1} - \omega^*_j T^j_{11} \right) + \sum_{j<k} \left(\omega_{jk} T^j_{1-1} - \omega^*_{jk} T^j_{11} \right) S_{kz}, \tag{11}$$

where it is assumed that spins j are of species I and spins k are of species S. Observation of the S-spin signal in the presence of $\mathrm{R}N_n^\nu$ irradiation on species I, followed by Fourier transformation, reveals a splitting due to the recoupled IS interactions.

Some preliminary results for the sequence $\mathrm{R18}_1^7$, with $\mathrm{R} = (180)_0$, are shown in Fig. 3. Written explicitly, the pulse sequence is

$$\mathrm{R18}_1^7 = \{(180)_{70}(180)_{-70}\}^9, \qquad (12)$$

where the superscript indicates 9 repetitions of the bracketed elements. The entire sequence of 18 $(180)_0$ pulses spans exactly one rotational period. Fig. 3a shows a ^{13}C spectrum of 98% -[2-^{13}C ,^{15}N]-L-alanine, with the signal acquired in the presence of repetitive $\mathrm{R18}_1^7$ sequences applied at the ^{1}H Larmor frequency. The ^{1}H nutation frequency was 90 kHz. The spectrum displays a clear three-peak structure, with the frequency separation of the outer components being 6.6 kHz. This splitting is due to recoupling of the heteronuclear interaction between the α–^{13}C and the attached proton during the acquisition of the ^{13}C signal. The central peak may be attributed to the simultaneous recoupling of the ^{1}H chemical shift anisotropy, which causes a partial decoupling effect for some molecular orientations [14]. The spectrum is in reasonable agreement with explicit spin dynamical simulations of an isolated ^{1}H–^{13}C system (Fig. 3b) using the COMPUTE algorithm [23].

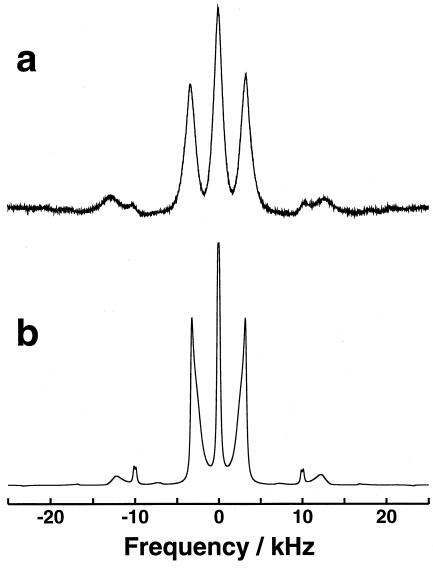

Fig. 3. (a) Experimental ^{13}C-MAS spectrum of 98% [2-^{13}C,^{15}N]-L-alanine at 9.4 T and a spinning frequency $\omega_r/2\pi = 10.0$ kHz. The ^{13}C magnetization was cross-polarized from the ^{1}H spins and the NMR signal acquired in the presence of a $\mathrm{R18}_1^7$ sequence applied to the protons, with a pulse element $\mathrm{R} = (180)_0$. The 6.6 kHz splitting between the two outer peaks is due to the recoupled ^{13}C–^{1}H dipolar interaction. (b) Numerically exact simulation of the ^{13}C spectrum of an isolated ^{13}C–^{1}H system, using a direct C–H coupling of $b_{\mathrm{IS}}/2\pi = -20.9$ kHz. The CSA of the ^{1}H site was assumed to be $\delta^{\mathrm{aniso}} = 1.25$ ppm, with $\eta = 0$ and with the principal axis aligned along the C–H bond.

We are currently exploring the applicability of these sequences for heteronuclear distance measurements [11,12,14,15], heteronuclear polarization transfer and multiple-quantum geometry determinations [16,24–27].

It is also possible to recouple heteronuclear dipolar interactions by combining $\mathrm{C5}_1^1$ symmetry with frequency-switched Lee–Goldburg irradiation [12,28].

5. Heteronuclear decoupling

In a recent paper [2], we applied $\mathrm{C}N_n^\nu$ sequences to the problem of heteronuclear decoupling. The $\mathrm{C}N_n^\nu$ sequences provide good heteronuclear decoupling if the symmetry numbers N, n and ν are chosen such that (i) there are no symmetry-allowed terms of the form $\overline{\mathscr{H}}^{(1)}_{2m1\mu}$; (ii) some terms of the form $\overline{\mathscr{H}}^{(1)}_{2m2\mu}$ are symmetry allowed; (iii) the number of terms of the form $\overline{\mathscr{H}}^{(2)}_{2m_21\mu_2;2m_11\mu_1}$ and $\overline{\mathscr{H}}^{(2)}_{2m_21\mu_2;2m_12\mu_1}$ is minimized. These conditions correspond to: (i) first order IS decoupling; (ii) first order II recoupling [2]; (iii) minimization of second order I $\times$ IS and II $\times$ IS cross terms. Sequences with appropriate properties include $\mathrm{C}N_2^1$, with $N \geqslant 11$. In particular, the sequence $\mathrm{C12}_2^1$ was found to have similar decoupling performance to TPPM [5] and performs consistently better than unmodulated rf irradiation ('continuous wave' or 'CW' decoupling).

Although the decoupling performance of $\mathrm{C12}_2^1$ may be rationalized within the framework of Eqs. (1) and (2), this theory provides no explanation for the good performance of TPPM, which does not have $\mathrm{C}N_n^\nu$ symmetry. The existing theories of TPPM [4,5] neglect the rotation of the sample and are of limited

utility for heteronuclear decoupling in rapidly rotating solids.

TPPM decoupling may be encompassed within the theory of RN_n^ν sequences, providing suitable synchronization conditions exist between the rf pulse scheme and the sample rotation. For example, the TPPM scheme $\pi_\phi\pi_{-\phi}$ with $\phi = 7.5°$ corresponds to the symmetry $R24_2^1$, if the rf field is adjusted to provide a nutation frequency $\omega_{\rm nut}^{\rm I} = 6\omega_r$. This corresponds to an I-spin nutation frequency of 90 kHz if the spinning frequency is 15 kHz. Similarly, the TPPM sequence $\pi_\phi\pi_{-\phi}$ with $\phi = 15°$ corresponds to the symmetry $R24_2^2$ under the same conditions. These are reasonable experimental parameters.

Under these synchronization conditions, it is possible to use the symmetry theorems to compare directly the TPPM sequences $R24_2^1$ and $R24_2^2$, with the sequence $C12_2^1$ and with unmodulated ('continuous-wave', CW) decoupling (which corresponds to $R24_2^0$ symmetry). All sequences use the same rf field amplitude if the basic element of the sequences are chosen to be $R = \pi_0$, while the basic element of the $C12_2^1$ sequence is chosen to be $C = (2\pi)_0$. Table 1 shows the results of this analysis. The table indicates that the principal differences between CW decoupling and the modulated schemes are: (i) the number of $I \times IS$ cross terms is reduced, attenuating the second-order recoupling effects [2,4]; (ii) some of the first order II coupling terms are restored. There is some evidence that this effect is also important for good heteronuclear decoupling [2–4]. Against these 'good' effects should be balanced: (iii) the number of $II \times IS$ cross terms is increased, which has a negative effect on the decoupling efficiency. Under most conditions, the beneficial effects (i) and (ii) outweigh the detrimental effect (iii) and lead to improved decoupling compared to CW.

If the modulated schemes are compared, we see that $C12_2^1$ and $R24_2^1$ are very similar, except that the number of symmetry-allowed $II \times IS$ cross terms is much smaller for the rotor-synchronized TPPM sequence $R24_2^1$. The TPPM scheme $R24_2^2$ appears to be inferior to $C12_2^1$ and $R24_2^1$ on most counts, except for the larger number of II terms in $\bar{\mathscr{H}}^{(1)}$.

The experimental results shown in Fig. 4 support this qualitative analysis. The displayed spectra are for a sample of [2,3-$^{13}C_2$]-L-alanine at a magnetic field of 9.4 T and a spinning frequency of 13 kHz.

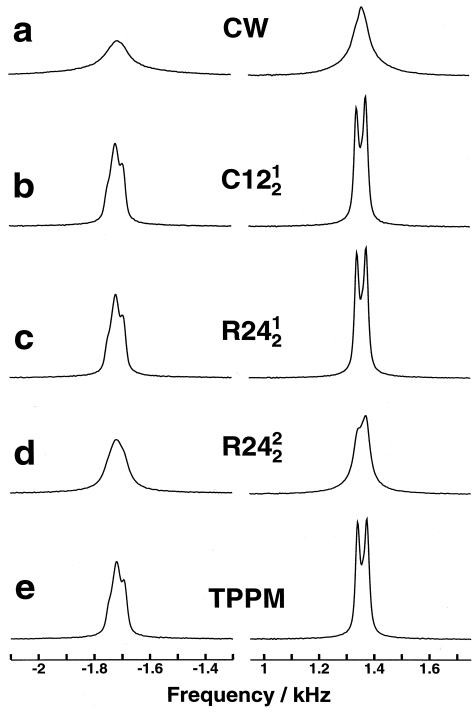

Fig. 4. Experimental ^{13}C spectra of 99% [2,3-$^{13}C_2$]-L-alanine at 9.4 T and a spinning frequency $\omega_r/2\pi = 13.0$ kHz using a filled 4 mm zirconia rotor. The spectra were obtained in the presence of different ^1H decoupling schemes: (a) CW, (b) $C12_2^1$ with $C = (2\pi)_0$, (c) $R24_2^1$ with $R = (\pi)_0$, (d) $R24_2^2$ with $R = (\pi)_0$, (e) TPPM with pulses of length 6.5 μs and $\phi = \pm 9°$. All sequences employed the same ^1H rf nutation frequency $\omega_{\rm nut}^{\rm I}/2\pi = 78$ kHz, corresponding to $\tau_C = 12.82$ μs for $C12_2^1$ and $\tau_R = 6.41$ μs for the R-sequences. All experiments employed on-resonance ^1H irradiation, except in the case of $C12_2^1$, where the rf reference frequency was offset by -6 kHz.

The pulse sequence is as described in Ref. [2], with appropriate substitution of the decoupling pulse sequence. The decoupling field corresponds to a nutation frequency of $|\omega_{\rm nut}^{\rm I}/2\pi| = 78$ kHz, matching the condition $\omega_{\rm nut}^{\rm I} = 6\omega_r$ as assumed in Table 1. Fig. 4a shows the ^{13}C spectrum in the presence of CW decoupling. The resolution is greatly improved by applying a $C12_2^1$ sequence (Fig. 4b). This reveals the $^{13}C-^{13}C$ J-coupling as a splitting, especially on the C3 (methyl) peak. A very similar spectrum is obtained with the rotor-synchronized TPPM sequence $R24_2^1$ (Fig. 4c). The similarity between Fig. 4b and Fig. 4c indicates that $II \times IS$ cross-terms do not appear to be very important, at least in this case. The

Table 1
Symmetry analysis of the rotor-synchronized TPPM sequences $R24_2^1$ and $R24_2^2$, the $C12_2^1$ sequence and CW decoupling ($R24_2^0$). All analyses are performed for the case $\omega_{nut}^I = 6\omega_r$, where ω_{nut}^I is the nutation frequency under the decoupling field and ω_r is the spinning frequency. The TPPM sequence $R24_2^1$ corresponds to repetition of the element $\pi_\phi\pi_{-\phi}$ with $\phi = 7.5°$. For the TPPM sequence $R24_2^2$, the phase shift is $\phi = 15°$. The sequence $C12_2^1$ corresponds to $(2\pi)_0(2\pi)_\phi(2\pi)_{2\phi}\ldots$ with $\phi = 30°$

Sequence	Symmetry	Number of symmetry-allowed terms			
		$\overline{\mathscr{H}}_{IS}^{(1)}$	$\overline{\mathscr{H}}_{II}^{(1)}$	$\overline{\mathscr{H}}_{I\times IS}^{(2)}$	$\overline{\mathscr{H}}_{II\times IS}^{(2)}$
CW decoupling	$R24_2^0$	0	0	24	0
TPPM with $\phi = 7.5°$	$R24_2^1$	0	2	8	16
TPPM with $\phi = 15°$	$R24_2^2$	0	4	16	44
$(2\pi)_0(2\pi)_{\pi/6}(2\pi)_{\pi/3}\ldots$	$C12_2^1$	0	2	8	36

resolution is much poorer for the rotor-synchronized TPPM sequence $R24_2^2$ (Fig. 4d). This is consistent with the higher number of $I \times IS$ cross-terms for $R24_2^2$, compared to $R24_2^1$ and $C12_2^1$ (Table 1).

This treatment is qualitative. A rigorous treatment of heteronuclear decoupling must take into account the form and magnitude of the symmetry-allowed terms, as well as their number. It may also be necessary to go to higher orders of the Magnus expansion. The selection rules (2) and (7) may be extended for this purpose, according to the results of Ref. [2].

There may be other ways of employing these selection rules to construct sequences with good heteronuclear decoupling properties. For example, the rotor-synchronized TPPM sequence $R26_2^3$ does not accomplish II recoupling but eliminates all $II \times IS$ cross-terms, at the same time as reducing the number of $I \times IS$ cross-terms to 8.

Practical implementations of TPPM often differ from the sequences described above in two respects: (i) usually, no care is taken to synchronize the rf pulse sequence with the sample rotation; (ii) the optimum flip angle for TPPM usually differs slightly from $\beta = 180°$. It is difficult to accommodate these adjustments in the existing symmetry theory of RN_n^ν sequences. Nevertheless, the following comments may be made: (i) although the existing theory is strictly invalid if the synchronization conditions are not met, the conclusions of the theory may still hold approximately for non-synchronized sequences. This is supported by the empirical observation that synchronization does not have a dramatic effect on the decoupling performance of TPPM, RN_n^ν and CN_n^ν sequences; (ii) deliberate misadjustments of pulse flip angles often have a beneficial effect on the heteronuclear decoupling efficiency. The effect is to induce additional rotation of the spin states which may average out some residual symmetry-allowed interactions. This was demonstrated explicitly for the $C12_2^1$ sequence in one case [2]. Clearly, more detailed work is necessary to evaluate the importance of non-synchronization and pulse missetting.

Fig. 4e shows that free optimization of the pulse duration and phase shift parameters for TPPM, without regard for maintaining RN_n^ν symmetry, does not significantly improve the decoupling performance, at least in this case. This supports the hypothesis that the performance of TPPM sequences may be understood quite well within the RN_n^ν symmetry framework.

6. Other applications

The RN_n^ν symmetries are powerful and permit the design of a wide range of rotor-synchronized pulse sequences with different properties. In particular, the participation of the spin rank λ in theorems (6) and (7) allows a clear distinction of chemical shift anisotropy ($\lambda = 1$) from homonuclear dipole–dipole interactions ($\lambda = 2$). This is not always possible in the framework of CN_n^ν symmetry, which only involves the quantum numbers m and μ.

The symmetries listed below are the results of a preliminary first-order analysis employing Eq. (6). Optimal solutions may be generated by studying the number of higher order terms using Eq. (7), and employing a detailed consideration of the properties of the element R.

6.1. Selection of J-couplings

Selective magnetization transfer through J-couplings ($l = 0,\ \lambda = 0$), suppressing chemical shift anisotropy ($l = 2,\ \lambda = 1$), isotropic chemical shifts ($l = 0,\ \lambda = 1$) and homonuclear dipole–dipole couplings ($l = 2,\ \lambda = 2$), may be achieved using $R6_1^0$ and $R8_1^0$ symmetries, as described by Baldus et al. [29]. These sequences are useful for assigning complex solid-state NMR spectra. The theorems given here allow the design of sequences which combine the properties listed above with rf inhomogeneity compensation. These include $R12_2^3$, $R14_3^5$ and $R12_4^5$. In total, 59 inequivalent symmetries have been found with $N \leqslant 20$ and $n \leqslant 5$. Some of these new symmetries may permit operation at high spinning frequencies. There are no CN_n^ν symmetries with all of the required properties.

6.2. Selection of isotropic chemical shifts

Isotropic chemical shifts ($l = 0,\ \lambda = 1$) may be selected, while suppressing all chemical shift anisotropy, homonuclear dipole–dipole coupling and rf inhomogeneity terms, by using a range of symmetries including $R6_1^3$, $R6_2^3$, $R8_3^4$. These sequences are likely to be useful for measuring isotropic chemical shifts in strongly-coupled homonuclear systems. In total, 27 inequivalent RN_n^ν symmetries have been found with $N \leqslant 20$ and $n \leqslant 5$. There are also 20 suitable CN_n^ν symmetries in the range $N \leqslant 10$ and $n \leqslant 5$, including $C6_1^3$, $C6_2^3$, $C8_3^4$. The symmetry $C3_1^0$ (which does not have intrinsic rf error compensation) was already pointed out by Demco et al. [30].

6.3. Single quantum homonuclear recoupling

In spin counting experiments [19,31,32], it may be desirable to construct an average Hamiltonian of the form:

$$\bar{\mathscr{H}}^{(1)} = \sum_{j<k} \left(\omega_{jk} T_{2-1}^{jk} - \omega_{jk}^* T_{21}^{jk} \right), \tag{13}$$

where T_{21}^{jk} and T_{2-1}^{jk} are second rank single-quantum spin operators for the dipolar coupling between spins j and k. The magnitude $|\omega_{jk}|$ is independent of the Euler angle γ_{MR}. The use of single-quantum spin operators allows spins to be counted in steps of one [31]. Engineering of this term, with first-order suppression of isotropic chemical shifts, chemical shift anisotropies and rf inhomogeneity terms, may be achieved by using the symmetries $R10_1^2$, $R14_2^4$, $R10_3^4$, $R14_4^8$. In total, 18 inequivalent RN_n^ν symmetries with suitable properties have been found in the range $N \leqslant 20$ and $n \leqslant 5$. There are no CN_n^ν symmetries with suitable properties.

6.4. Orientationally-encoded homonuclear recoupling

Internuclear distances in multiple spin systems may be estimated by using recoupling sequences with a complicated dependence on the molecular orientation [33]. The coherencies created by such sequences carry a characteristic orientation-dependence which causes distance-dependent modulations in certain two-dimensional experiments. However, the sequences proposed so far have been sensitive to chemical shifts. It is possible to exploit RN_n^ν symmetries to engineer orientation-dependent dipolar recoupling, at the same time as first-order suppression of isotropic and anisotropic chemical shift terms as well as suppression of rf inhomogeneity terms. Some examples are $R8_1^1$, $R6_2^2$, $R8_3^3$, $R6_4^2$. A total of 27 suitable symmetries has been found with $N \leqslant 20$ and $n \leqslant 5$. There are no CN_n^ν symmetries with suitable properties.

6.5. Zero-quantum dipolar recoupling

An average Hamiltonian proportional to T_{20}^{jk} may be engineered in magic-angle spinning NMR by using the symmetry $R4_4^1$. This is the only solution in the range $N \leqslant 20$ and $n \leqslant 5$ which combines T_{20}^{jk} selection with first-order removal of rf inhomogeneity and chemical shift terms. Sequences with $R4_4^1$ symmetry provide an alternative to the RIL pulse sequence [29] and should be functional at high spinning frequencies.

6.6. Simultaneous double-quantum and CSA recoupling

Recoupling of dipolar interactions and CSA terms at the same time allows one to determine the relative

orientation of spin interaction tensors [34]. $\mathrm{R}N_n^\nu$ symmetries allow simultaneous recoupling to be achieved while compensating the pulse sequence for isotropic chemical shifts and rf amplitude missets. A particularly desirable form for the recoupled average Hamiltonian is

$$\bar{\mathscr{H}}^{(1)} = \sum_j \left(\omega_j T^j_{1-1} - \omega_j^* T^j_{11} \right) + \sum_{j<k} \left(\omega_{jk} T^{jk}_{2-2} + \omega^*_{jk} T^{jk}_{22} \right), \quad (14)$$

where the magnitudes $|\omega_j|$ and $|\omega_{jk}|$ and the relative phases of ω_j and ω_{jk} are independent of the Euler angle γ_{MR}. Some symmetries of this type are $\mathrm{R}8^3_1$, $\mathrm{R}10^1_2$, $\mathrm{R}8^1_3$, $\mathrm{R}18^4_5$. A total of 25 suitable $\mathrm{R}N_n^\nu$ symmetries has been found in the range $N \leqslant 20$ and $n \leqslant 5$. There are no suitable $\mathrm{C}N_n^\nu$ symmetries.

6.7. Heteronuclear applications

There are also numerous possibilities involving multiple-channel rf irradiation, which will be explored in future publications.

7. Conclusions

We have described a new set of symmetry theorems which provide a flexible framework for the construction of rotor-synchronized rf pulse sequences with a wide range of properties. We have applied these theorems to the design of homonuclear and heteronuclear dipolar recoupling sequences and shown how the new symmetry theorems provide insight into the mechanism of TPPM decoupling. In addition, new symmetries have been proposed for many other recoupling and decoupling problems in solid-state NMR.

Acknowledgements

This research was supported by the Swedish Natural Science Foundation and by the Göran Gustafsson Foundation for Research in the Natural Science and Medicine. Andreas Brinkmann was supported by a Marie Curie Research Training Grant ERBFMBICT961439 from the European Union. We would like to thank Ole G. Johannessen for experimental help, Angelika Sebald and Heidi Maisel for the sample of diammonium $^{13}C_2$-fumarate and Huub de Groot for a copy of Ref. [17] prior to publication.

References

[1] M. Mehring, Principles of High Resolution NMR in Solids, Springer, Berlin, 1983.
[2] M. Edén, M.H. Levitt, J. Chem. Phys. 111 (1999) 1511.
[3] P. Tekely, P. Palmas, D. Canet, J. Magn. Res. Series A 107 (1994) 129.
[4] M. Ernst, S. Bush, A.C. Kolbert, A. Pines, J. Chem. Phys. 105 (1996) 3387.
[5] A.E. Bennett, C.M. Rienstra, M. Auger, K.V. Lakshmi, R.G. Griffin, J. Chem. Phys. 103 (1998) 6951.
[6] A.E. Bennett, R.G. Griffin, S. Vega, NMR Basic Principles and Progress 33 (1994) 1.
[7] Y.K. Lee, N.D. Kurur, M. Helmle, O.G. Johannessen, N.C. Nielsen, M.H. Levitt, Chem. Phys. Lett. 242 (1995) 304.
[8] M. Hohwy, H.J. Jakobsen, M. Edén, M.H. Levitt, N.C. Nielsen, J. Chem. Phys. 108 (1998) 2686.
[9] C.M. Rienstra, M.E. Hatcher, L.J. Mueller, B. Sun, S.W. Fesik, R.G. Griffin, J. Am. Chem. Soc. 120 (1998) 10602.
[10] A. Brinkmann, M. Edén, M.H. Levitt, J. Chem. Phys. (2000), accepted for publication.
[11] T. Gullion, J. Schaefer, Adv. Magn. Res. 13 (1989) 57.
[12] J.D. Gross, P.R. Costa, R.G. Griffin, J. Chem. Phys. 108 (1998) 7286.
[13] S. Dusold, A. Sebald, Ann. Rep. NMR Spectrosc. 41 (2000), in press.
[14] M.H. Levitt, T.G. Oas, R.G. Griffin, Isr. J. Chem. 28 (1988) 271.
[15] T.G. Oas, R.G. Griffin, M.H. Levitt, J. Chem. Phys. 89 (1988) 692.
[16] M.H. Levitt, D.P. Raleigh, F. Creuzet, R.G. Griffin, J. Chem. Phys. 92 (1990) 6347.
[17] B.-J. van Rossum, C.P. de Groot, V. Ladizharsky, S. Vega, H.J.M. de Groot, J. Am. Chem. Soc. (2000), in press.
[18] M. Edén, M.H. Levitt, Chem. Phys. Lett. 293 (1998) 173.
[19] O.N. Antzutkin, R. Tycko, J. Chem. Phys. 110 (1999) 2749.
[20] U. Haeberlen, J.S. Waugh, Phys. Rev. 175 (1968) 453.
[21] M.H. Levitt, R. Freeman, J. Magn. Res. 43 (1981) 502.
[22] A.J. Shaka, A. Pines, J. Mag. Res. 71 (1987) 495.
[23] M. Edén, Y.K. Lee, M.H. Levitt, J. Magn. Res. A 120 (1996) 56.
[24] X. Feng, Y.K. Lee, D. Sandström, M. Edén, H. Maisel, A. Sebald, M.H. Levitt, Chem. Phys. Lett. 257 (1996) 314.
[25] X. Feng, M. Edén, A. Brinkmann, H. Luthman, L. Eriksson, A. Gräslund, O.N. Antzutkin, M.H. Levitt, J. Am. Chem. Soc. 119 (1997) 12006.
[26] Y. Ishii, T. Terao, M. Kainosho, Chem. Phys. Lett. 265 (1996) 133.

[27] P.R. Costa, J.D. Gross, M. Hong, R.G. Griffin, Chem. Phys. Lett. 280 (1997) 95.
[28] A. Bielecki, A.C. Kolbert, H.J.M. de Groot, R.G. Griffin, M.H. Levitt, Adv. Magn. Res. 14 (1990) 111.
[29] M. Baldus, R.J. Iulicci, B.H. Meier, J. Am. Chem. Soc 119 (1997) 1121.
[30] D.E. Demco, S. Hafner, H.W. Spiess, J. Magn. Res. A 116 (1995) 36.
[31] D. Suter, S.B. Liu, J. Baum, A. Pines, Chem. Phys. 114 (1987) 103.
[32] Y. Yen, A. Pines, J. Chem. Phys. 78 (1983) 3579.
[33] J. Gottwald, D.E. Demco, R. Graf, H.W. Spiess, Chem. Phys. Lett. 243 (1995) 314.
[34] M. Bak, N.C. Nielsen, J. Chem. Phys. 106 (1997) 7587.
[35] W.S. Veeman, Progr. NMR Spectr. 16 (1984) 193.